Tribology International 197 (2024) 109822

Contents lists available at ScienceDirect

Tribology International

journal homepage: www.elsevier.com/locate/triboint

Full Length Article

Engineering tribological rehydration of cartilage interfaces: Assessment of potential polyelectrolyte mechanisms

Robert J. Elkington [a,*], Richard M. Hall [b], Andrew R. Beadling [a], Hemant Pandit [c], Michael G. Bryant [b]

[a] Institute of Functional Surfaces, Mechanical Engineering, University of Leeds, Leeds, LS2 9JT, Yorkshire, UK
[b] School of Engineering, College of Engineering and Physical Sciences, University of Birmingham, Birmingham, B15 2TT, West Midlands, UK
[c] Leeds Institute of Rheumatic and Musculoskeletal Medicine, Chapel Allerton Hospital, Chapeltown Road, Leeds, LS7 4SA, Yorkshire, UK

ARTICLE INFO

Keywords:
Polyelectrolyte surfaces
Cartilage
Tribological rehydration
BioTribology

ABSTRACT

Articular cartilage, primarily composed of water and collagen, is vital for synovial joint function. Traditional hard biomaterials like ceramic or cobalt-chrome used in hemiarthroplasty often result in abnormal contact pressures and premature implant failure. This study investigates the tribological properties of polyelectrolyte functionalised PEEK (SPMK-g-PEEK) in contact with cartilage, proposing a solution to these issues by utilising tribological rehydration and effective aqueous lubrication.

We demonstrate a new mode of polyelectrolyte enhanced tribological rehydration where SPMK-g-PEEK achieves low friction and promotes interstitial fluid recovery during sliding, independent of traditional hydrodynamic theories. This results in a rapid stabilisation of the coefficient of friction (CoF) to levels comparable to natural cartilage (CoF ~ 0.01) and aids in approximately 8% cartilage strain recovery, indicating effective tribological rehydration even under cartilage degradation or altered osmotic conditions.

Furthermore, we find that lubrication and rehydration against an SPMK-g-PEEK interface depend minimally on biphasic lubrication but significantly on the hydrophilic sulfonic acid groups of SPMK, which act as a fluid reservoir. Our findings suggest SPMK-g-PEEK as a promising biomaterial for cartilage interfacing implants that offer low friction and modulate cartilage interstitial fluid pressure. This study enhances our understanding of biotribological interactions and contributes to the development of joint replacement materials that support the natural function of cartilage.

1. Introduction

Early intervention ahead of total joint replacement necessitates material systems capable of repairing articular cartilage defects, which are present in 80% of symptomatic osteoarthritis cases, to restore native synovial joint function and mitigate degenerative cartilage loss [1]. However, the current use of hard biomaterials, such as ceramics or cobalt chromium molybdenum (CoCrMo) alloys, in hemiarthroplasty or focal repair devices is inappropriate for articulation against the soft, compliant nature of articular cartilage. Often leading to abnormally high contact pressures which can promote erosion of mating cartilage, leading to premature implant failure and costly revision surgeries [2–4]. Finite element models have enabled simulations of stresses and fluid pressures in physiological joints, revealing the drawbacks of hard, impermeable materials currently used in hemiarthroplasty such as CoCrMo. These materials reduce contact area, compromise fluid load support, and increase collagen matrix stress [5,6]. Consequently, biotribological and medical device researchers are increasingly focusing on soft biphasic materials to support cartilage fluid loads along with maintaining suitable friction and stress.

In order to develop biomimetic materials for the next generation of cartilage interfacing focal joint repair implants, it is essential to understand healthy synovial joint tribology. Articular cartilage is an 80% water and 20% collagen porous fibril matrix with a hierarchical architecture enriched with proteoglycans [7], which relies on two key lubrication mechanisms: biphasic and boundary-mediated. The biphasic nature of cartilage governs load distribution and fluid film formation. Key processes include boosted and weeping lubrication [8,9], fluid load support [10], and tribological rehydration [11]. Interstitial fluid pressure are hypothesised to support up to 90% of the joint load, mitigating collagen matrix overload [12,13]. *In vivo* studies indicate that periodic joint activity sustains fluid pressurisation, reducing strain and friction at the cartilage interface [14–16]. MRI data show that

* Corresponding author.
E-mail address: mnrje@leeds.ac.uk (R.J. Elkington).

https://doi.org/10.1016/j.triboint.2024.109822
Received 26 January 2024; Received in revised form 9 May 2024; Accepted 23 May 2024
Available online 24 May 2024

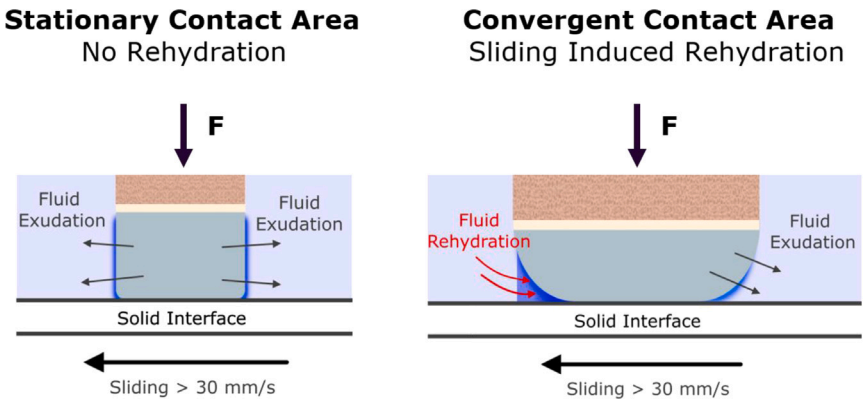

Fig. 1. Schematic of tribological rehydration for a Stationary Contact Area (SCA) which exhibits no rehydration and a convergent Stationary Contact Area (cSCA) which provides a pressurised convergent leading edge to facilitate fluid entrainment and rehydration.

in vivo knee strain in healthy humans ranges from 5%–10% during gait [17]. Boundary-mediated lubrication is provided by an adsorbed boundary film composed of biopolyelectrolytes like hyaluronic acid, and glycoproteins including lubricin and aggrecan, as well as surface-active phospholipids [18–20]. A key feature of this system is hydration lubrication, which arises from the hydrophilic domains within these molecules. These domains bind water molecules tightly, forming stable hydration shells which rapidly exchange water ions between opposing groups to dissipate friction [20–23]. This mechanism is critical because it facilitates a low-friction, self-healing interface, thereby enhancing joint mobility and reducing wear on cartilage at low speeds.

Cartilage exhibits dynamic biphasic behaviour *in vivo*, requiring interstitial fluid flow and pressurisation to recover and respond to loading conditions during joint articulation in order to maintain lubricity and safe levels of collagen loading [24]. Initial theories suggested that cartilage rehydration occurred through free swelling during unloading [8]. Later, Ateshian's work clarified that a migrating contact area helps maintain fluid pressure by constantly providing hydrated tissue at the interface [25,26]. Recently, Burris and Moore introduced a concept called *Tribological Rehydration*, a hydrodynamically-driven mechanism that replenishes interstitial fluid in cartilage during sliding [11,27]. Effective tribological rehydration requires a convex cartilage interface which provides convergent contact area and sliding speeds exceeding 30 mm s^{-1} to generate hydrodynamic pressures that overcome the cartilage interstitial fluid pressure, facilitating rehydration [28–31].

Fig. 1 illustrates the required geometry for a convergent Stationary Contact Area (cSCA) that facilitates tribological rehydration. This rehydration is driven by hydrodynamic effects generated by a wedge-shaped inlet at the contact's leading edge [27,32]. In contrast, a Stationary Contact Area (SCA) without a convergent inlet exhibits behaviour analogous to unconfined compression during sliding, wherein fluid continues to be exude from the cartilage. Experiments show that cartilage plugs with small diameters, providing only a SCA, lack rehydration capabilities. This results in the breakdown of biphasic lubrication and fluid load support, leading to increased friction [27].

Functional bearing surfaces suitable for articulating against cartilage must provide a highly hydrated interface which can both provide hydration lubrication at the boundary, and a pressurised water reservoir to facilitate cartilage rehydration. Hydrogels, biphasic soft materials and polymer brushes are garnering significant interest in the field of cartilage mimetics and focal lesion repair. These materials can be engineered to match the viscoelastic mechanical properties of cartilage together with their high water content to exhibit an analogous physical state to cartilage [33,34]. The inherent poroviscoelasticity of hydrogels is beneficial for fluid pressurisation under mechanical loads, contributing to fluid load support and biphasic lubrication mechanisms. However, the typically larger pore sizes found in hydrogels, in contrast to the finer porosity of cartilage, lead to diminished fluid load support and inferior creep behaviour, indicating a biomechanical mismatch [35,36]. Furthermore, challenges related to the fixation of hydrogel materials to articular surfaces pose significant hurdles for their clinical application, necessitating further research to resolve these issues before clinical deployment [37,38].

Polymer brushes, particularly those based on 2-methacryloyloxyethyl phosphorylcholine (MPC) and 3-sulfopropyl methacrylate potassium salt (SPMK) are of interest as a bioinspired surface coating which resemble highly hydrated biomacromolecules (e.g. hyaluronic acid and lubricin) found in synovial fluid and adsorbed on the cartilage surface [39–41]. The zwitterionic phosphorylcholine group of MPC, and anionic sulfonic acid group of SPMK, are highly hydrophilic and are surrounded with tenaciously bound hydration shells [40,42]. Electrostatic repulsion between the charged groups is able to maintain the brush conformation at pressures exceeding 100 MPa [43]. Hydrophilic polymer brushes in aqueous environments can facilitate hydration lubrication due to the high content of tenaciously bounded hydration shells [40,42]. Polymer brushes are able to provide a high degree of lubricity along with highly hydrated interface in environments and at loads akin to a physiological synovial joint. Tribological studies of polymer brush interfaces sliding against cartilage remain limited. One study demonstrated that CoCrMo surfaces functionalised with MPC brushes could achieve friction coefficients <0.01 and in pin-on-plate tests of 5000 cycles showed no damage to the cartilage collagen structure following histological analysis, providing an early indication for applications in hemiarthroplasty [44].

Recent research has introduced modified PEEK surfaces functionalised with SPMK (SPMK-g-PEEK) as a 350 nm thick hydrophilic coating rich in anionic sulfonic acid groups [45]. SPMK is a biocompatible surface treatment [46], which when used as an orthopaedic implant coating for articulating against cartilage can actively support tissue hydration [47]. Tribological testing against SCA bovine cartilage demonstrates that SPMK-g-PEEK maintains low friction, minimises cartilage strain, and reduces stress at the cartilage interface. Notably, SPMK-g-PEEK was found to increase cartilage's effective interfacial permeability during sliding and support a greater interstitial fluid equilibrium, exhibited as a reduced cartilage strain [45,48]. SPMK-g-PEEK sliding against cartilage provides fluid recovery through polyelectrolyte enhanced tribological rehydration, where compression of the swollen SPMK polyelectrolyte provides localised fluid pressurisation, which rehydrates the interfacing cartilage [47].

This study aims to elucidate the underlying mechanisms governing cartilage rehydration mediated by SPMK-g-PEEK and explore different tribological and adverse physiological conditions to examine the suitability of polyelectrolyte modified implant surfaces for synovial joint repair. By employing a flat SCA cartilage area (Fig. 1), no converging entrainment zone is present at the cartilage interface, meaning any cartilage rehydration observed is independent of conventional hydrodynamic tribological rehydration facilitated by a convergent wedge geometry [11].

2. Materials and methodology

2.1. Materials

PEEK 450G (Victrex, UK), acquired from RS Components (UK), was obtained as 5 mm thick flat sheets and sectioned into 25 × 25 mm square samples. 3-Sulfopropyl methacrylate potassium salt (SPMK) monomer with a purity exceeding 98% and phosphate-buffered saline tablets were sourced from Sigma Aldrich (UK) and used as received.

All PEEK samples underwent a sequential polishing regimen to achieve a target surface roughness (R_a) of 100 nm. The protocol entailed progressive grinding with abrasive papers of P240, P400, P800, and P1200 grits, succeeded by final polishing using diamond and silica oxide suspensions with particle sizes ranging from 3 to 0.04 μm. Following polishing, surface topography was validated using a Talysurf PGI NOVUS profilometer.

2.2. Tissue samples

Cartilage plugs, each 7.2 mm in diameter, were extracted from the patellofemoral grooves of bovine stifle joints acquired from John Penny & Sons, Leeds, UK. The selected specimens originated from bovines that were sacrificed for a food distribution service, consequently it is not possible to record a precise age and hence had an age range associated with 1–2 years old.

A high-speed (35,000 rpm) rotary tool fitted with an 7.2 mm internal diameter trephine bur and cooled with a steady stream of phosphate-buffered saline (PBS) was employed for plug extraction. During the harvesting process, each cartilage plug underwent a thorough inspection for visible defects and geometric inconsistencies. To ensure uniformity in the subsequent analyses, plugs displaying greater than 0.2 mm height difference across the cartilage surface were systematically excluded to maintain consistency in sample geometry across the study. The samples were cryopreserved (−18 °C) in PBS and thawed at least 12 h prior to testing in a refrigerated environment, followed by acclimatisation to room temperature for an additional 2 h immedietely before testing.

2.3. UV photopolymerisation

Fig. 2 demonstrates the UV initiated atom transfer radical polymerisation (ATRP) workflow by which 3-Sulfopropyl methacrylate potassium salt (SPMK) was grafted onto the surface of polished PEEK samples to produce SPMK-g-PEEK [45,49,50]. The PEEK samples are initially cleaned with acetone and isopropanol before submersion in a 1 mol L^{-1} SPMK oxygen free aqueous solution. Substrates are then placed in a UV Crosslinker (Analytik Jena UVP Crosslinker CL-3000L) at 365 nm wavelength for 90 min, achieving a total UV exposure of 27 J cm^{-2}. The one-step polymerisation leverages the self-initiating capability of PEEK's benzophenone units, eliminating the need for an external photoinitiator. The resulting SPMK-g-PEEK surfaces end tethered polyelectrolyte interface possess anionic sulfonic acid groups, providing a hydrophilic, lubricious interface favourable for biotribological applications. Detailed methodologies and associated chemistry are elaborated in our prior publication on SPMK-g-PEEK [45].

2.4. Mechanical testing

A Bruker UMT Tribolab equipped with a reciprocating linear drive and a custom lubricant bath was employed for cartilage-pin tribological assessment against unfunctionalised PEEK and SPMK-g-PEEK plates. The testing apparatus fully submerged samples in phosphate-buffered saline (PBS) to simulate physiological osmotic conditions, thereby mitigating cartilage swelling and sustaining a hydrated equilibrium analogous to an *in vivo* environment. Closed-loop control concurrently measured the Coefficient of Friction (μ) and the compressed cartilage height of cartilage (Δh) to calculate real-time strain, ϵ:

$$\mu = \frac{F_x}{F_z} \tag{1}$$

$$\epsilon = \frac{\Delta h}{h} \tag{2}$$

where F_x and F_z denote the measured forces in the tangential and normal directions respectively, and h is the measured fully swollen height of the cartilage.

Throughout this study, only 7.2 mm diameter cartilage plugs were used, this was determined to be the largest cartilage plug that can be harvest from bovine condyles and still provide a SCA (Fig. 1) [45]. This is necessitated by the requirement to minimise any contribution of tribological rehydration borne through convergent wedge effects, in order to observe alternative mechanisms of tribological rehydration. Similarly during sliding tests a low speed of 10 mm s^{-1} was used to further minimise rehydration from previously described hydrodynamic effects.

Fig. 3 shows the rehydration cycle testing protocol used to determine cartilage strain recovery after a period of interstitial fluid loss. The protocol consists of an initial 30-min compression phase, succeeded by a 30-min compression-sliding phase at a linear reciprocating velocity of 10 mm s^{-1} over a sliding distance of 20 mm. Importantly, the cartilage remains under a constant normal load (F_z) of 30 ± 3 N throughout the test, regulated via PID control. This load corresponds to a physiologically relevant contact pressure of approximately 0.75 MPa [51,52].

Post-testing, cartilage pins were stored and prepared using standardised protocols before undergoing height measurements [45]. Cartilage height was measured using a calibrated Keyence VHX-7000 microscope at 20× zoom. A series of images were captured to provide a comprehensive 360° view of the cartilage layer to yield a precise mean cartilage height, calculated using Keyence's software to provide an average cartilage height h. For the evaluation of mechanical properties, Coefficient of Friction (CoF) and strain were averaged over the mid 50% of each reciprocating cycle to assess steady-state sliding conditions. Strain response, characterised as viscoelastic time-dependent creep, was analysed through a custom Python 3.7 script based on a standard linear solid model.

2.5. Experimental overview

To comprehensively understand the tribological behaviour of SCA cartilage against PEEK and SPMK-g-PEEK a systematic series of experiments were performed. The scope encompassed analysing the rehydration cycle (Fig. 3) for PEEK and SPMK-g-PEEK surfaces against freshly harvested and damaged cartilage samples, with inhibited rehydration, and for an overlapping 'unreplenished' contact zone. The methodologies adopted for each experimental condition, along with the underlying rationale, are discussed in the subsequent sections, and the specific experimental conditions are concisely summarised in Table 1. To ensure repeatability experiments were conducted triplicate (n = 3) for each test condition to ascertain average CoF and strain evolution during throughout the rehydration cycle.

Rehydration cycle

PEEK and SPMK-g-PEEK were tested against undamaged 7.2 mm SCA cartilage plugs undergoing the rehydration cycle defined in Fig. 3 in PBS lubricant. This experiment provides the preliminary assessment of the compression recovery and tribological performance between the unfunctionalised PEEK and SPMK modified surfaces.

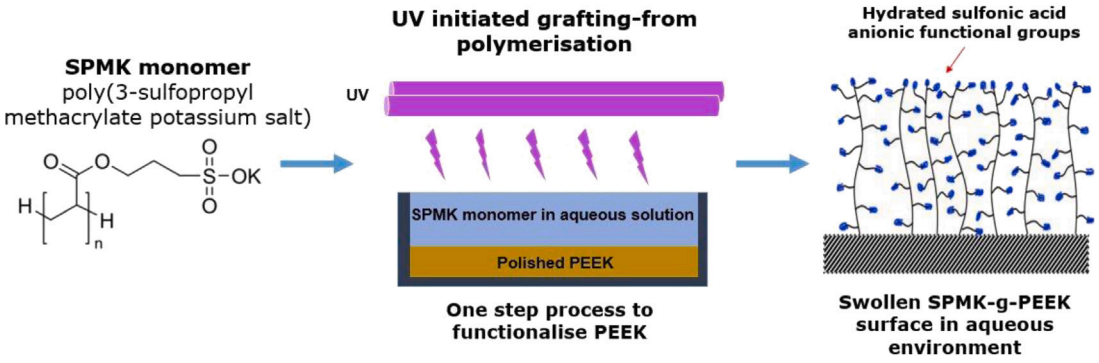

Fig. 2. SPMK-g-PEEK workflow. SPMK monomer is dissolved at a 1 mol L^{-1} concentration in deionised water. The polished PEEK sample is then submerged in the aqueous SPMK solution and undergoes UV (365 nm) photopolymerisation for 90 min at an intensity of 5 mW cm^{-2}. Following grafting, the SPMK-g-PEEK sample is washed under a stream of deionised water to remove any unreacted monomer.

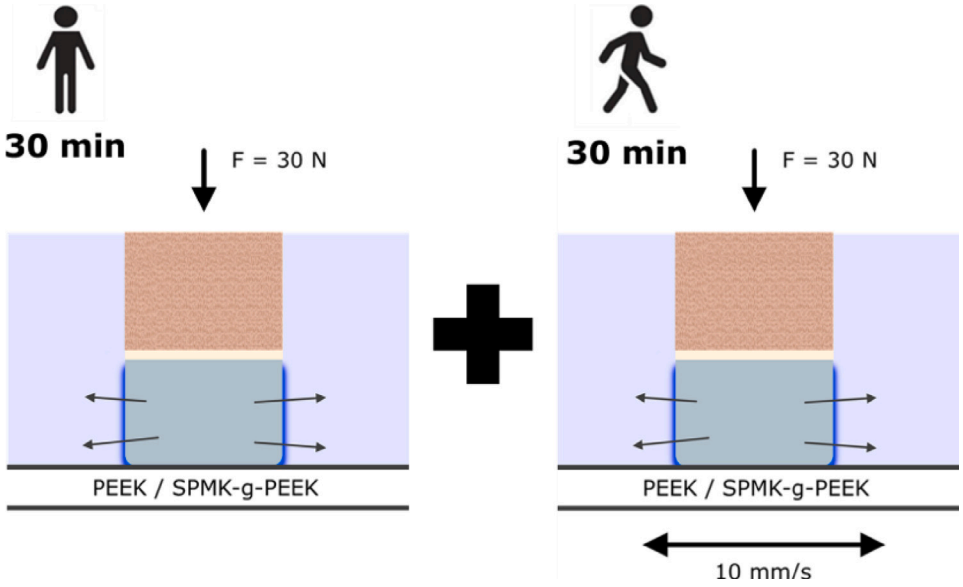

Fig. 3. Schematic of the cartilage pin on plate UMT testing showing the physiological testing protocol of the compression (30 min) and compression-sliding (30 min) cycles.

Table 1
Summary of experimental conditions for the Rehydration Cycle, Abraded Cartilage, Inhibited Rehydration, and Overlapping SCA datasets. Every experiment underwent the rehydration cycle loading profile (Fig. 3b) and all experiments were conducted triplicate (n = 3) for each distinct set of conditions.

Experiment	Interface	Cartilage	Lubricant	Stroke length
Rehydration cycle	-PEEK-SPMK-g-PEEK	Undamaged	PBS	20 mm
Abraded cartilage	-PEEK-SPMK-g-PEEK	Abraded	PBS	20 mm
Diminished rehydration	SPMK-g-PEEK	Undamaged	2M NaCl	20 mm
Overlapping SCA	SPMK-g-PEEK	Undamaged	PBS	1 mm 3.5 mm 7 mm

Abraded cartilage

SCA cartilage plugs were abraded using 250 μm grit paper, undergoing a 600 mm traversal while altering the orientation of the cartilage surface. This technique was employed to ensure the generation of a non-directional, uniformly damaged surface profile [53,54]. Removal of the superficial zone is analogous to a situation of early cartilage degradation, and from a biomechanical perspective provides a more porous interface [53,55]. Both PEEK and SPMK-g-PEEK surfaces underwent the rehydration cycle against damaged SCA cartilage to understand the fluid recovery mechanics of damaged tissue.

Diminished rehydration

Rehydration cycles were performed in a 2 ML^{-1} NaCl solution to impose a substantial osmotic gradient to inhibit rehydration and biphasic tribology of cartilage. This condition aims to isolate the contribution of hydration lubrication at the SPMK interface by inhibiting interstitial fluid recovery thus limiting the contribution of biphasic lubrication.

Overlapping SCA

Hydrogel and cartilage lubrication theories demonstrate that limiting hydration at the sliding interface through a short reciprocating overlapping stroke results in starvation of the contact area, consequently leading to elevated friction [56,57]. Concentrating on a confined 'overlapping' regime, characterised by a stroke length shorter than the contact width, facilitates the investigation of the lubrication efficacy of SPMK-g-PEEK in an overlapped contact, analogous to the operational conditions of numerous physiological joints [57]. During overlap, the SPMK surface remains constantly constrained to prevent free swelling, thereby challenging the optimal hydration of the polyelectrolyte interface. Investigating different reciprocating lengths of 1,

Table 2
Consolidated data reflecting the Startup CoF (μ_S), Final CoF (μ_F), strain post-compression (ε_C), and post-sliding (ε_F), along with the recovered strain ($\varepsilon_r = \varepsilon_C - \varepsilon_F$) for the sliding (rehydration) phase, encompassing all experiments summarised in Table 1.

Test	μ_S (–)	μ_F (–)	ε_C (%)	ε_F (%)	ε_r (%)
Rehydration cycles					
PEEK	0.234 ± 0.069	0.378 ± 0.021	40.72 ± 1.97	49.10 ± 3.05	−8.39 ± 1.24
SPMK-g-PEEK	0.010 ± 0.003	0.005 ± 0.001	41.02 ± 7.33	32.10 ± 5.90	8.05 ± 1.21
Abraded					
PEEK	0.188 ± 0.076	0.298 ± 0.073	34.34 ± 5.15	38.25 ± 3.53	−3.91 ± 1.76
SPMK-g-PEEK	0.014 ± 0.001	0.006 ± 0.001	35.89 ± 2.84	23.82 ± 4.84	12.06 ± 1.96
Diminished rehydration					
NaCl - SPMK-g-PEEK	0.012 ± 0.002	0.005 ± 0.001	45.44 ± 4.94	43.83 ± 6.21	1.61 ± 1.72
Overlapping SCA					
1 mm	0.022 ± 0.015	0.004 ± 0.004	39.90 ± 2.79	33.88 ± 2.25	6.01 ± 0.58
3.5 mm	0.012 ± 0.002	0.009 ± 0.004	40.42 ± 5.31	32.16 ± 7.19	7.43 ± 1.71
7 mm	0.012 ± 0.007	0.008 ± 0.005	44.98 ± 9.82	36.41 ± 9.53	7.79 ± 0.68

3.5, and 7 mm enabled comparison of varying degrees of contact area overlap, in particular a non-replenished 'overlapping' regime where the stroke length is shorter than the contact width (1 mm and 3.5 mm sliding distances). For each test a peak velocity of 10 mm s^{-1} is maintained over the duration of the 1800 s sliding phase, hence for each test a total sliding distance of 18 m is achieved.

3. Results

Following unconfined compression and resultant interstitial fluid exudation from the cartilage, the initiation of sliding produced markedly low CoF of less than 0.01 when articulated against SPMK-g-PEEK samples. This was accompanied by notable interstitial fluid re-uptake and corresponding strain recovery. The summarised data for the Startup CoF (μ_S), Final CoF (μ_F), strain post-compression (ε_C), final strain post-sliding (ε_F), and recovered strain ($\varepsilon_r = \varepsilon_C - \varepsilon_F$) across rehydration cycles are presented in Table 2 highlighting the key experimental findings for tests defined in Table 1. The uncertainty values represent one standard deviation for CoF and strain at the start of sliding$t$ = 1800 s (μ_S & ε_C respectively) and CoF and strain at the end of the sliding-rehydration phase at t = 3600 s (μ_F & ε_F respectively). The recovered strain (ε_r) is calculated as the mean strain recovery and standard deviation across each repeated rehydration cycle. The high standard deviation for strain values reflect the mechanical and poroviscoelastic variability of cartilage samples across unique bovine specimens and patellofemoral location of harvesting, these are consistent with previous studies of cartilage tribology with strain uncertainties of >±5% [58,59].

3.1. Rehydration cycles

As illustrated in Fig. 4, the behaviour of SCA cartilage in contact with unfunctionalised PEEK (Fig. 4(a)) and SPMK-g-PEEK (Fig. 4(b)) during the rehydration cycles reveals distinct differences in compression recovery and tribological efficacy. At the onset of sliding cartilage SCA sliding against PEEK did not exhibit any compression recovery, rather exhibiting an additional 8.39 ± 1.24% further strain as interstitial fluid continued to be irreversibly efflux under load, yielding a final strain of ε_F = 49.1 ± 3.05%. Concurrently, the friction increases from an initial μ_S = 0.23 ± 0.07 up to μ_F = 0.38 ± 0.02 at the end of the test without reaching a steady equilibrium. The increasing strain and CoF during sliding indicates a continuing breakdown in biphasic lubrication, inhibiting hydration at the interface and loss of interstitial fluid pressurisation. Conversely, for SPMK-g-PEEK the cartilage strain recovered by 8.05 ± 1.21% during sliding, demonstrating re-uptake of interstitial fluid upon the onset of sliding for a final reduced strain of ε_F = 32.1 ± 5.9%. The hydrated interface facilitates a low startup μ_S = 0.01 ± 0.003 and rapidly decreased to a stable CoF of μ_F = 0.005 ± 0.001 throughout the majority of the 30 min sliding cycle.

3.2. Abraded cartilage

Fig. 5 shows the rehydration cycle for cartilage which has been abraded with sandpaper to simulate damaged cartilage, sliding against PEEK (Fig. 5(a)) and SPMK-g-PEEK (Fig. 5(b)). In relation to the healthy cartilage benchmarks in Fig. 4(a), abraded cartilage sliding against PEEK exhibits reduced post compression strain of ε_C = 34.3 ± 5.2% which upon the onset of sliding continues to increase at a reduced rate towards a final strain of ε_F = 38.3 ± 3.5%, culminating in a ε_r increase of 3.91 ± 1.8%. The startup μ_S = 0.19 ± 0.08 is comparable to the undamaged cartilage case, and increases quickly towards a quasi-steady and final μ_F = 0.30 ± 0.07.

Abraded cartilage sliding against SPMK-g-PEEK recovers a greater fraction of cartilage strain (ε_r = 12.1 ± 2.0%) compared to the undamaged control in Fig. 4(b). The CoF trend matches the healthy cartilage benchmark, with a startup μ_S = 0.01 ± 0.001 quickly stabilising to a final equilibrium μ_F0.006 ± 0.001. Demonstrating that for a scenario where cartilage has been biomechanically diminished, SPMK-g-PEEK still provides an interface that can support the biphasic and hydrated boundary tribology of cartilage.

3.3. Diminished rehydration

Fig. 6 shows the average compression and friction data for the rehydration cycle of cartilage against SPMK-g-PEEK immersed in a 2 ML^{-1} NaCl solution to inhibit the rehydration of articular cartilage. The high osmotic gradient of the salt solution likely contributed to the high strain following the compression phase (ε_C = 45.4 ± 4.9%), and also minimal strain recovery during sliding where interstitial fluid recovery was inhibited, resulting in a recovery of only ε_r = 1. 6 ± 1.7% but nonetheless during sliding the SPMK-g-PEEK did facilitate cartilage rehydration. The frictional characteristics are consistent with those observed for SPMK-g-PEEK in a phosphate-buffered saline (PBS) control environment (Fig. 4(b)). Initial startup friction initiates at μ_S = 0.01 ± 0.002 and swiftly plateaus to a stable μ_F = 0.005 ± 0.001.

3.4. Overlapping contact area

Fig. 7 displays the mean strain and frictional response for three distinct stroke lengths, 1 mm, 3.5 mm, and 7 mm, corresponding to the sliding phase of the rehydration cycle, as depicted in Fig. 3. These profiles exemplify three unique contact configurations characterised by different degrees of overlap, enabling assessment of whether SPMK-g-PEEK can effectively promote cartilage rehydration and enhance lubrication whilst the SPMK polyelectrolyte interface is constrained from free-swelling between strokes.

Strain recovery for both the overlapped (1 mm, 3.5 mm stroke) and non-overlapped (7 mm stroke) conditions exhibit comparable CoF behaviour with low startup μ_S between 0.03 – 0.01, and in all cases

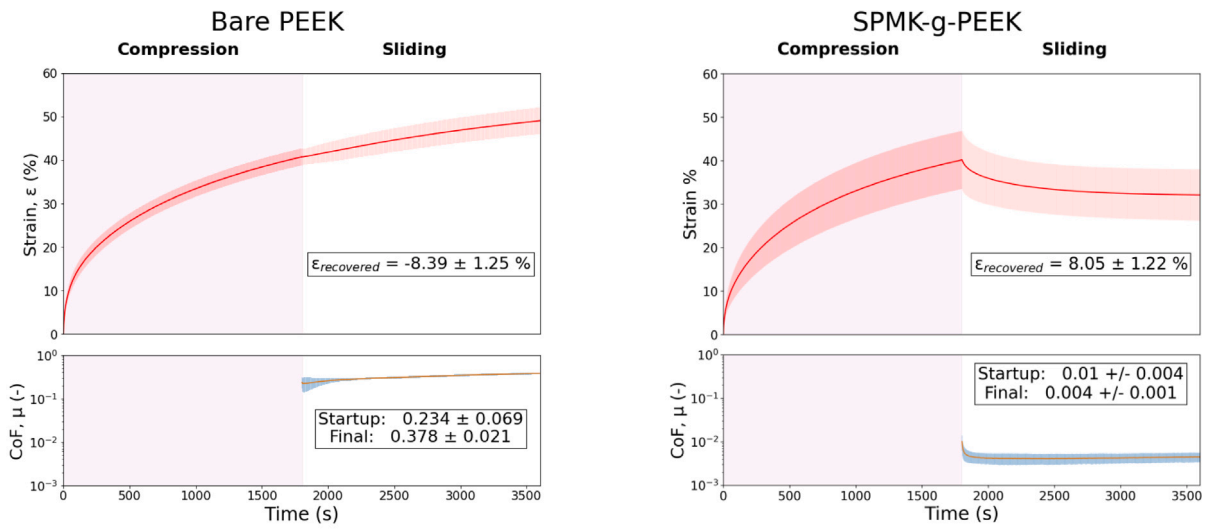

(a) PEEK (b) SPMK-g-PEEK

Fig. 4. Compression and CoF data for the rehydration cycles of (a) unfunctionalised PEEK (n = 3) showing no evidence of rehydration upon the onset of sliding and (b) SPMK-g-PEEK (n = 3) showing strain recovery upon sliding.

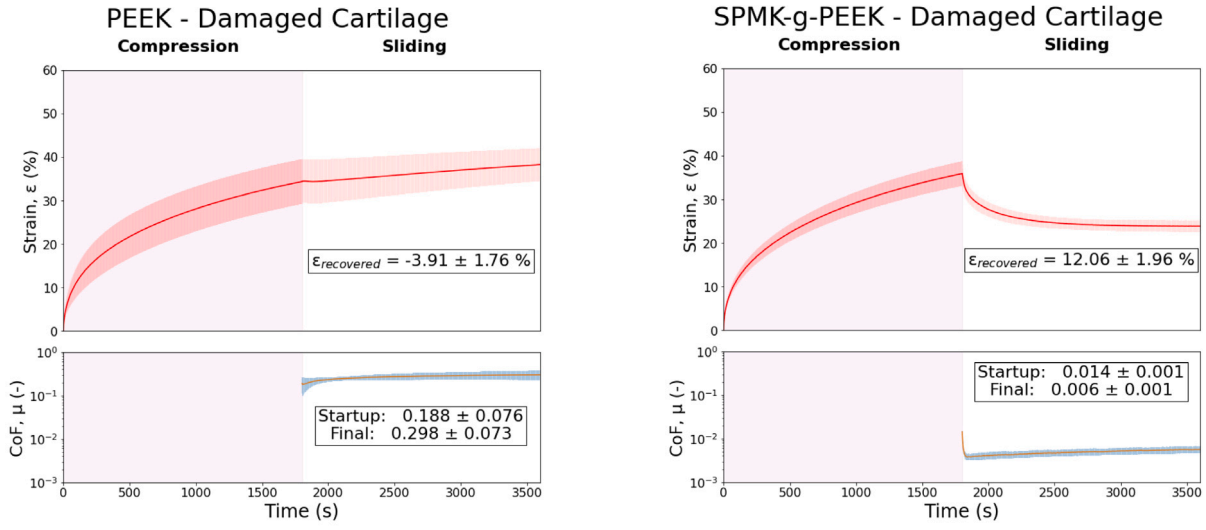

(a) PEEK (b) SPMK-g-PEEK

Fig. 5. Compression and CoF data for the rehydration cycles of (a) unfunctionalised PEEK (b) SPMK-g-PEEK against cartilage samples that have been abraded with 250 μm grit sandpaper.

rapidly reaching a sustained steady state CoF with $\mu_F < 0.01$. Total strain recovery during sliding was commensurate with increasing sliding distance. The shortest 1 mm reciprocating distance exhibited the lowest $\varepsilon_r = 6.0 \pm 0.6\%$, followed by 3.5 mm sliding with $\varepsilon_r = 7.4 \pm 1.7\%$, and finally 7 mm sliding $\varepsilon_r = 7.8 \pm 0.7\%$. Compared to the 20 mm stroke rehydration cycle (Fig. 4(b)) which exhibited $\varepsilon_r = 8.1 \pm 1.2\%$, the predominantly overlapped condition of 1 mm sliding showed a reduced ability to recover interstitial fluid.

4. Discussion

This study elucidates the efficacy of SPMK-g-PEEK to facilitate low friction and modulate cartilage hydration through a novel mechanism of tribological rehydration. Our findings reveal that SPMK-g-PEEK significantly enhances strain recovery during sliding consistently in the conditions outlined. Soft biomimetic interfaces may be a key advance in biomaterials utilised within articulating surfaces for joint prostheses, addressing the limitation of conventional polymeric and metallic surfaces that fail to emulate the intrinsic biphasic and hydrated tribology of articular cartilage. The subsequent sections will delineate the promising performance of the SPMK-g-PEEK - cartilage interface and the mechanisms underlying the SPMK polyelectrolyte ability to maintain low friction and facilitate interstitial fluid recovery.

4.1. SPMK-g-PEEK tribological rehydration

By employing a rehydration cycle (Fig. 3) it was possible to directly observe and quantify compression recovery of cartilage during sliding. Unfunctionalised PEEK demonstrated continued compression at the onset of sliding, characteristic of a cartilage SCA which provides no entrainment zone for fluid recovery, subsequently throughout the test CoF continued to increase as biphasic lubrication diminished, depriving the contact area of lubricating interstitial fluid [27]. This yielded an increasing CoF of 0.23 up to 0.38, which is consistent with previous 30–60 min tests for SCA cartilage sliding against a hard planar counter-face [10,25,60].

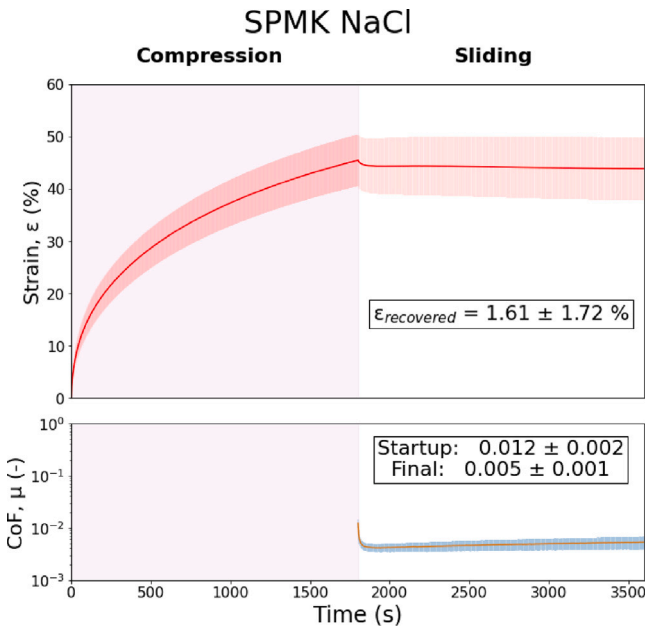

Fig. 6. Compression and CoF data for the rehydration cycle of SPMK-g-PEEK samples submerged in 2 ML^{-1} NaCl water to inhibit fluid flow.

For the same SCA configuration with SPMK-g-PEEK, cartilage was able to re-uptake interstitial fluid during sliding characterised by a reduced strain along with a rapidly stabilised μ_F of 0.005. SPMK-g-PEEK surfaces provide an interface with performance akin to natural cartilage-cartilage biomechanics [25]. Notably, even in adverse conditions where the surface of cartilage has been abraded or the rehydration has been inhibited by an osmotic gradient, SPMK-g-PEEK continued to facilitate low CoF of ~0.01 at the interface along with tribological rehydration to reduce overall strain. The low friction coefficients achieved in this study are the same magnitude as MPC functionalised Co-Cr-Mo sliding against cartilage [44]. Whilst this previous study briefly postulates that the MPC polymer brush provides a water source for rehydration of cartilage contributing to a sustained low CoF, our findings go a step further by providing empirical evidence of the rehydration mechanism through direct observation of cartilage strain recovery, a process underpinned by a highly hydrated multiphase interface composed of hydrophilic polyelectrolytes.

The CoF and strain recovery observed in this study for the SPMK-g-PEEK and SCA cartilage contact pair are similar in magnitude to studies by Burris on tribological rehydration of cSCA cartilage on glass [58,59]. Adopting a similar rehydration protocol of 30 min compression followed by 30 min sliding, strain recovery (ε_r) was reported between 3% and 7%, initially presenting relatively high startup CoF of 0.17–0.20 before settling to lower equilibrium CoF of 0.03–0.06 [58,59]. However, in these studies all tribological rehydration was contingent on a cSCA cartilage plug and high speeds of 80 mm s^{-1}, which facilitates fluid entrainment borne through convergent wedge hydrodynamics [11,30]. Contrasting with these findings, the SPMK-g-PEEK-mediated rehydration demonstrated in this study occurs under flat SCA conditions and at significantly reduced speeds (10 mm s^{-1}). This observation not only expands the conventional scope of tribological rehydration but also suggests alternative mechanisms at play beyond convergent wedge hydrodynamic entrainment.

The low friction achieved by tethered polyelectrolytes is lower than cartilage-cartilage contacts in a migrating contact geometry (MCA), which exhibit steady state CoF in the range 0.02–0.04 along with tribological rehydration [25,61]. While our study corroborates the rehydration that underpins biphasic lubrication for cartilage interfaces, for SPMK-g-PEEK the markedly lower startup CoF and rapid approach to equilibrium CoF of less than 0.01 can be attributed to the inherent low friction characteristics of hydration shells which provide a highly lubricious aqueous interface [62].

The consistency of low CoF and rehydration, irrespective of healthy cartilage biomechanical function, underscores the promising tribological properties of SPMK-g-PEEK as a material choice for cartilage interfacing implant surfaces for patients with early-stage cartilage disease. In this study, the observed peak cartilage strains of approximately 30%–40% are significantly higher than the typical *in vivo* strains of 5%–10% [17]. However, prior research indicates that strains within this range do not compromise the mechanical integrity of the cartilage [63]. Additionally, a previous study investigating SCA cartilage interfaced with SPMK-g-PEEK under identical loading conditions reported no cartilage fibrillation after 2.5 h of sliding [45]. Therefore, these higher strains likely do not introduce an error related to damage in the collagen matrix when examining tribological rehydration post-compression. Effective tribological rehydration has been shown to mitigate cartilage cell death by supporting a high fluid load fraction and lubricity [64]. Elevated fluid pressurisation not only reduces friction but also provides essential mechanical support to cartilage, mitigating degenerative effects often seen in early stage cartilage disease [65,66].

4.2. Role of polyelectrolyte lubrication

SPMK polyelectrolyte interfaces are innately lubricious due to the hydrophilic sulfonic acid groups which facilitate hydration lubrication [43]. This explains the overall lower startup CoF (<0.02) observed for all tests against SPMK-g-PEEK, compared to previous experiments on cSCA cartilage against glass which exhibited startup CoF of 0.17–0.20 [58,59].

Conventional understanding of sustained cartilage lubrication requires competing interstitial fluid recovery to closely match efflux, sustaining interstitial fluid pressure and a constant supply of lubricant at the cartilage interface. For a MCA or cSCA contact configuration, the temporal CoF response of cartilage in sliding ($\mu(t)$) can be represented as a function of solid phase friction (μ_s) and the interstitial fluid load fraction ($\frac{W_f(t)}{F_z}$) shown in Eq. (3) [60,67]. This relationship demonstrates that low friction can only be sustained with a high degree of interstitial fluid pressure, which has a non-linear relationship to cartilage strain [67,68].

$$\mu(t) = \mu_s(1 - \frac{W_f(t)}{F_z}) \tag{3}$$

However, the impeded rehydration of cartilage against SPMK-g-PEEK conducted in 2 ML^{-1} NaCl (Fig. 6) only recovered 1.6% strain throughout sliding whilst rapidly stabilising a low friction of 0.005, the same CoF evolution observed for SPMK-g-PEEK in PBS where uninhibited rehydration recovered 8.4% strain (Fig. 4(b)). The presence of surface tethered SPMK polyelectrolytes offers a persistent boundary lubricant with viscous fluid characteristics [69,70]. This indicates that the lubrication performance of SPMK-g-PEEK against cartilage is primarily controlled by the highly hydrated SPMK polyelectrolyte interface, with a minimal reliance on the effectiveness of biphasic lubrication arising from interstitial pressurisation.

4.3. Mechanism of polyelectrolyte enhanced tribological rehydration

After the compression phase, the strain (ε_C) in both PEEK and SPMK-g-PEEK samples was approximately 40%, as shown in Table 2. This result indicates that the presence of the SPMK interface does not influence interstitial fluid efflux under static conditions. The rehydration of these materials only occurs upon the initiation of sliding, suggesting that the SPMK-g-PEEK interface activates a dynamic lubrication mechanism that is not reliant on alterations to the porosity of the cartilage. Specifically, the sliding motion appears to generate sufficient fluid pressure to overcome the interstitial fluid pressure of the cartilage,

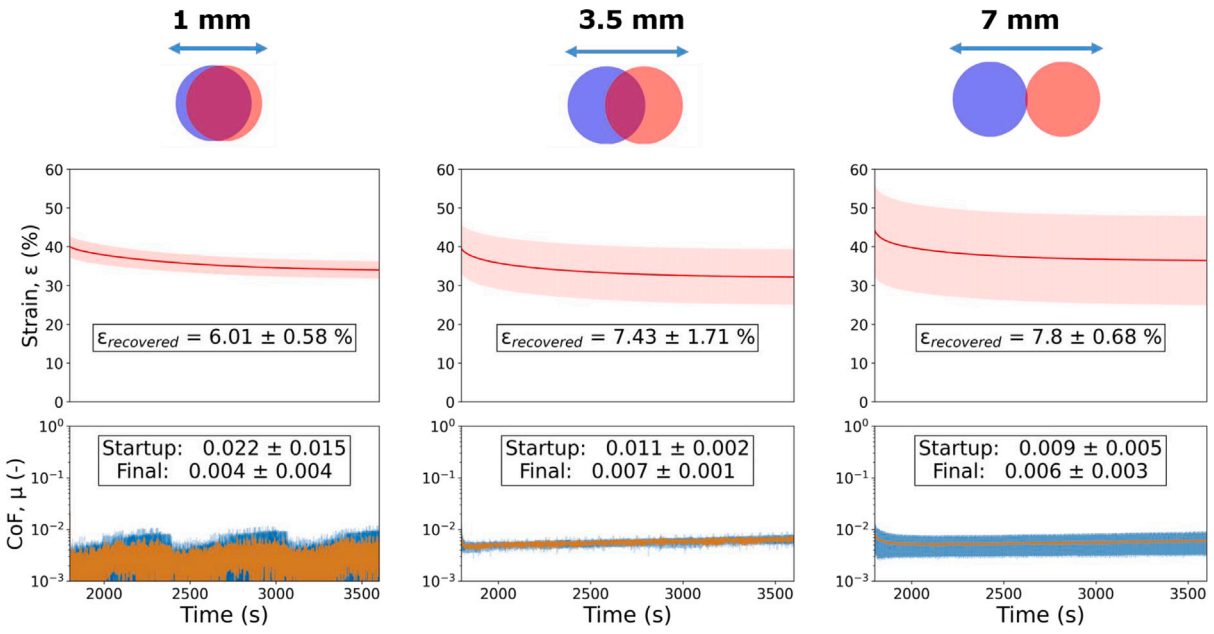

Fig. 7. Compression and CoF data for the just the sliding phase of the rehydration cycle for sliding with a stroke length of (a) 1 mm (b) 3.5 mm (c) 7 mm.

thereby facilitating fluid ingress towards a reduced strain equilibrium. This tribological rehydration mechanism, observed in experiments using a flat SCA cartilage contact model, deviates from the mechanisms described in existing literature, which typically involve hydrodynamic pressurisation at a convergent inlet in models using a larger curved cSCA cartilage contact [11,30].

Primarily, the presence of a swollen, highly hydrated polyelectrolyte layer acts as a replenishing source of water, thus facilitating the rehydration of articular cartilage [45]. The mechanisms underlying polyelectrolyte enhanced tribological rehydration of cartilage is hypothesised to be a combination of micro elastohydrodynamic lubrication (μEHL) and polyelectrolyte enhanced elastohydrodynamic lubrication (PB-EHL) [47,69,71]. Established theories of μEHL theories suggest that the surface roughness of cartilage, which has a relatively low elastic modulus, is smoothed by two orders of magnitude under modest loading conditions. This smoothing effect facilitates the formation of a fluid film, enabling effective lubrication at the cartilage contact [71–73].

Polyelectrolytes and gel layers substantially enhance elastohydrodynamic lubrication (EHL) film thickness and lower the transition speed required to achieve an EHL regime in aqueous lubrication [23,74]. Optical interferometry tribological assessments of various hydrophilic polymer brush interfaces reveal that these materials maintain a stable aqueous film approximately 30–35 nm thick at low entrainment speeds (around 10^{-3} mm s^{-1}), attributed to the hydration effects of the polymer brushes [75,76]. At speeds increase to ~10^{-2} mm s^{-1}, a low speed transition is observed to a PB-EHL regime with fluid films rapidly expanding up to 100 nm thick [69,76]. Contrasting to classical EHL theories which necessitate viscous lubricants for a separating fluid film. In aqueous systems, the presence of a swollen polymer brush layer itself can behave as a viscous lubricant to produce PB-EHL at low speeds [23,43,75–77]. This aligns with previous observations of SPMK-g-PEEK polyelectrolyte enhanced tribological rehydration. Showing effective rehydration from speeds at velocities as low as 0.5 mm s^{-1} with a progressively increasing degree of rehydration correlating with speeds up to 10 mm s^{-1}, consistent with the speed-dependent evolution of EHL [47]. At the nanoscale, it is hypothesised that compression of the swollen, hydrophilic SPMK polyelectrolyte concentrates water molecules, thereby enhancing EHL formation through increased fluid pressurisation [45,47].

Fig. 8 shows the proposed lubrication regime for polyelectrolyte enabled tribological rehydration. At regions of μEHL fluid film formation, the PB-EHL enhanced viscosity of the water lubricating layer may give rise to a fluid pressure gradient. Nearest the outlet of the contact where the fluid pressure (P_F) is the highest and overcomes the interstitial fluid pressure of cartilage ($P_F > P_{IFP}$) water can be recovered by the cartilage, leading to tribological rehydration and overtime reducing the overall strain of cartilage during sliding. The presence of polyelectrolytes can reduce the speeds required for the evolution of EHL lubrication fluid films and due to the enhanced local viscosity, PB-EHL can give rise to greater local fluid pressures and thicker fluid films than water alone. This is akin to a mode of boosted lubrication, whereby the presence of biological macromolecular polyelectrolytes native to synovial fluid (i.e. hyaluronic acid, lubricin) in the contact gap can increase viscosity leading to enhanced hydrodynamic pressurisation at reduced speeds [78–80]. Biological polyelectrolyte constituents of synovial fluid have been widely compared to polymer brush tribology, providing both a highly effective boundary lubricant and affinity to maintain fluid film lubrication [81,82]. For SPMK-g-PEEK, instead of relying on entrainment and confinement of polyelectrolytes, the SPMK is tethered to the PEEK substrate providing unabating boosted lubrication localised at the contacting asperities of the SCA cartilage counterface [47].

For SPMK-g-PEEK sliding against an SCA cartilage plug the total strain recovery plateaued following an exponential decay in total strain until a reduced strain equilibrium is reached. For undamaged PEEK sliding at 10 mm s^{-1} the total recovery was $\varepsilon = 8.1 \pm 1.2\%$ demonstrating a mechanistic limit to overall strain recovery of cartilage. The hypothesis presented here posits an equilibrium state is reached between the fluid film pressure, denoted as P_F, and the interstitial fluid pressure of cartilage, P_{IFP}. Cartilage mimicking early signs of degradation the cartilage abraded with 250 μm grit sandpaper exhibits a greater overall strain recovery (Fig. 5(b), $\varepsilon_r = 12.1 \pm 2.0\%$) compared to the undamaged control (Fig. 4(b), $\varepsilon_r = 8.1 \pm 1.2\%$). Suggesting that the rougher, abraded cartilage surface will yield higher local asperity pressurisation leading to increased local fluid pressures and hence a greater degree of cartilage interstitial fluid recovery.

4.4. Effect of overlapping contact on rehydration

Hydrogel and cartilage lubrication requires the contact area to remain hydrated, for short distance reciprocating contacts exhibiting

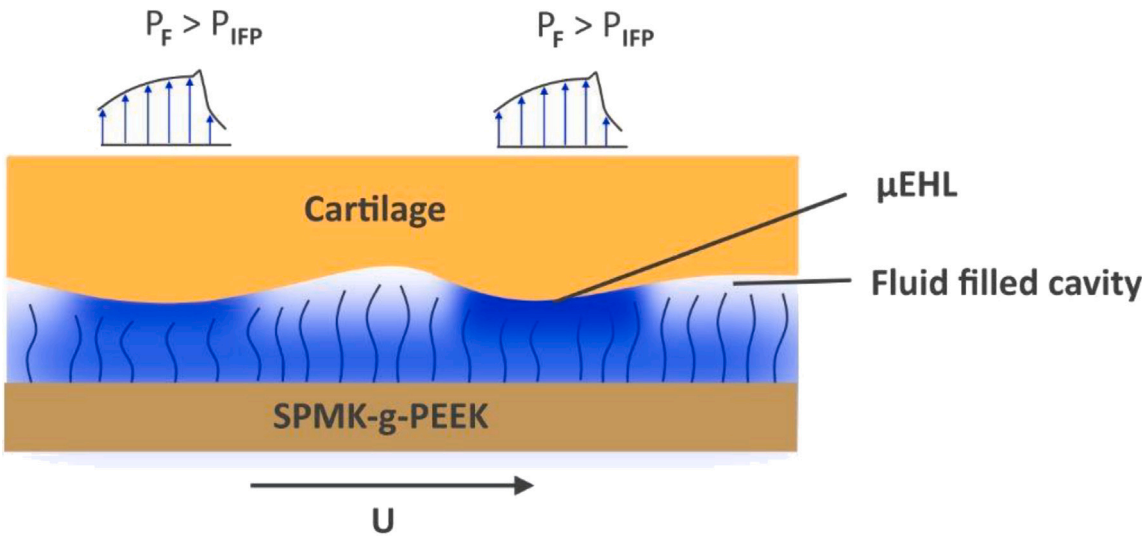

Fig. 8. Proposed lubrication regime showing cartilage deformation giving rise to local regions of μEHL where a polyelectrolyte enhanced fluid film is present. Postulating where the fluid pressure is greatest (P_F) this overcomes the interstitial pressure of the cartilage ($P_F > P_{IFP}$) fluid can be imbibed back into cartilage, facilitating polyelectrolyte enhanced tribological rehydration.

an overlapping contact area, friction characteristically increases as the lubricant is unreplenished in the overlapped sliding area [56,57]. Similarly, polymer brush tribology relies heavily on sustained hydration to ensure lubricity [43,69]. Additionally, under compressive forces, surfaces functionalised with polyelectrolytes undergo dehydration, leading to a partial collapse of the brush structure, a reduction in water volume, and consequently, increased friction [83,84].

Testing overlapped contact areas (Fig. 7) demonstrates reduced strain recovery for the overlapped 1 mm sliding distance $\varepsilon_r = 6.0 \pm 0.6\%$ compared to the $\varepsilon_r \sim 8\%$ for longer sliding distances. Upon modelling the strain recovery time constant (τ) using a single-phase exponential decay function (Eq. (4)), the 1 mm stroke condition corresponding to the greatest overlap area exhibits a protracted recovery time of $\tau = 611$ s. In contrast, the 7 mm (Fig. 7c) and 20 mm (Fig. 4(b)) non-overlapped conditions demonstrate nearly equivalent, and notably shorter, rehydration times of 358 s and 384 s respectively shown in Fig. 9. Despite the reduced strain recovery (τ) for the 1 mm overlapping contact condition, CoF still remains characteristically low, with startup and rapid stabilisation to the final CoF observed for all conditions ~0.01 (Fig. 7). This suggests that the hydrophilic SPMK polyelectrolyte, even under persistent compression in the overlapped sliding area, maintains a substantial water content, thereby providing an effective swollen lubricating interface. Similar ATRP produced polymer brush interfaces (MPC & SPMK) with hydrophilic functional groups necessitate pressures of above 100 MPa before dehydration and subsequent breakdown of lubricity occurs [85,86]. For SPMK the tenaciously bound hydration shells due to the anionic sulfonic acid groups can effectively resist dehydration under the 0.75 MPa physiological contact pressures used in this study.

The rehydration of the cartilage is hypothesised to arise from a synergistic effect of augmented fluid films, attributable to PB-EHL, in conjunction with the water-retentive properties of the hydrophilic SPMK polyelectrolyte, which acts as a fluid reservoir for rehydration. The observed diminution in overall rehydration and the decelerated strain recovery rate associated with shorter overlapping stroke lengths can likely be attributed to the incomplete formation of the fluid film. Conventional hydrodynamic film development necessitates a stroke length exceeding twice the contact width for full fluid film development [57,87]. Nevertheless, notable cartilage rehydration is observed even at the minimal 1 mm reciprocating distance, with ε_r recorded at $6.0 \pm 0.6\%$, suggesting that the rehydration mechanism is predominantly facilitated by the hydrophilic SPMK, which serves as an effective fluid reservoir.

$$\varepsilon_{rehydration}(t) = \varepsilon_C + \varepsilon_r \cdot e^{\left(\frac{-t}{\tau}\right)} \tag{4}$$

4.5. Limitations & future work

Comparative clinical data suggest that healthy knee cartilage should experience strains between 5%–10% during gait activities [17], whereas the equilibrium strain observed with SPMK-g-PEEK implants was approximately 30%. Whilst a major finding of this study is the novel demonstration of polyelectrolyte tribological rehydration, it is necessary to understand the cumulative strain recovery through a combined cSCA/MCA and SPMK-g-PEEK tribological study. We speculate that the combined tribological rehydration effects of a conformal or convergent contact geometry and the boosted cartilage rehydration facilitated by SPMK-g-PEEK could closer emulate physiological cartilage interstitial fluid mechanics and support.

The scope of this paper honed in on empirical evidence of polyelectrolyte mediated cartilage strain recovery, with experiments designed to elucidate the underpinning roles of hydration lubrication and contact dynamics which reimbibe fluid into cartilage. As such, all experiments have been performed in hour long tests in a contact configuration unlike the conformal geometry of synovial joints. In order to escalate technology readiness, longer tests will be performed along with physiological duty cycles (e.g. gait) to understand the long term performance and potential failure mechanisms of SPMK-g-PEEK.

Finally, Section 4.3 which explores the PB-EHL mechanism of tribological rehydration relies on EHL theory developed for classical engineering bearings, non-aqueous systems, or confined polymer brush systems [69,77,87]. Whilst contextualisation of this study against the aforementioned literature provides insight into the SPMK contact dynamics, there exists a gap in the literature that fully encapsulates the complex tribological interplay observed in this research. The interface formed by polyelectrolyte surfaces interfaced with cartilage requires an intricate model encompassing the permeable poroviscoelastic mechanics of cartilage along with the macromolecular and nanorheological dynamics of SPMK. PB-EHL is a plausible hypothesis for the observed cartilage rehydration, an upcoming study will seek to further validate the PB-EHL hypothesis across a range of speeds and contact configurations.

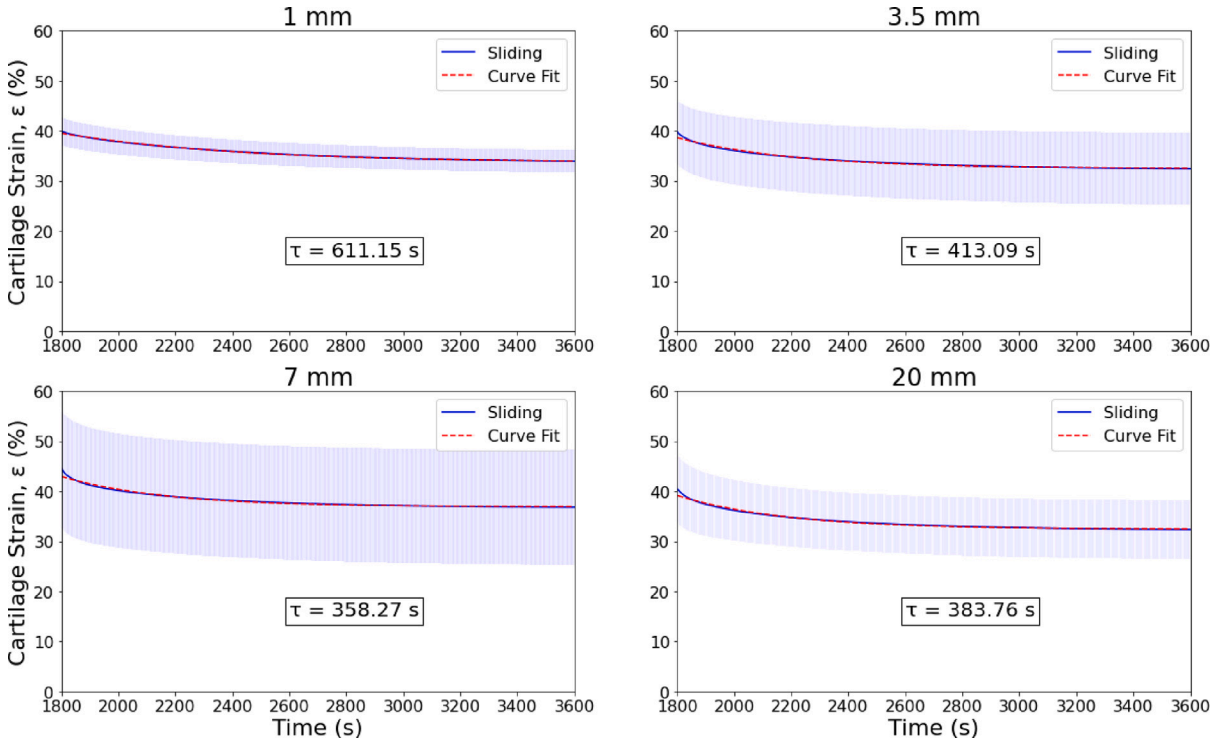

Fig. 9. Rate of tribological rehydration strain recovery τ calculated for 1 mm, 3.5 mm, 7 mm, and 20 mm reciprocating distances for SCA cartilage against SPMK-g-PEEK.

5. Conclusions

Three key characteristics of SPMK-g-PEEK have been identified which elucidate the unique demonstration of sustained lubrication and tribological rehydration for a flat stationary contact area cartilage plug. Firstly, the SPMK polyelectrolyte provides a boundary lubricant which provides a highly hydrated viscous lubricious interface, and against cartilage offers a highly lubricious counter-face even in absence of biphasic lubrication. Secondly, the high density of surface tethered hydrophilic sulfonic acid groups provides an aqueous reservoir as a source for cartilage interstitial fluid recovery. And thirdly, tribological rehydration is facilitated by polyelectrolyte enhanced elastohydrodynamic lubrication, akin to boosted lubrication, where the surface tethered SPMK enhance the local viscosity to provide substantial pressurised fluid films.

This study presents SPMK-g-PEEK as a compelling biocompatible coating for orthopaedic implants articulating against cartilage. Providing support for the native biomechanics of articular cartilage, offering both low friction $\mu \sim 0.01$ along with enhanced interstitial fluid load support and cartilage strain recovery of ~8%. Notably, SPMK-g-PEEK maintains consistent tribological performance even under conditions where cartilage surfaces are damaged or incapable of sustaining normal interstitial fluid homeostasis. The SPMK polyelectrolyte interface provides further insight into modes of tribological rehydration beyond prevailing theories contingent on high speed, convergent geometry hydrodynamic lubricant pressurisation [25,27,57].

SPMK-g-PEEK surface exhibits lubrication characteristics that surpass traditional hydrodynamic and biphasic lubrication models, achieving lower friction coefficients at reduced sliding speeds. This expands the scope of tribological applications to include conditions where high-speed fluid entrainment is not feasible, such as in low-mobility patients or in smaller planar joints where large articulating motions are limited. The tribological performance of synthetic polymers in contact with cartilage has substantial implications for orthopaedic applications, particularly for the next generation of hemiarthroplasty and focal cartilage resurfacing. Furthermore, this has expanded the scope of mechanisms underpinning tribological rehydration and highlights the substantive tribological efficacy of hydrophilic macromolecules, providing further insight into the role of biopolyelectrolytes, such as lubricin and hyaluronic acid, in synovial biotribology.

Data avaliability

The data associated with this paper are openly available from the Mendeley Data repository. Available: Elkington, Rob (2024), "Engineering tribological rehydration of cartilage interfaces: Assessment of potential polyelectrolyte mechanisms", Mendeley Data, V1, doi: 10.17632/mfpycfwyrh.1.

CRediT authorship contribution statement

Robert J. Elkington: Writing – review & editing, Writing – original draft, Visualization, Validation, Supervision, Software, Resources, Methodology, Investigation, Formal analysis, Data curation, Conceptualization. **Richard M. Hall:** Writing – review & editing, Supervision. **Andrew R. Beadling:** Writing – review & editing, Supervision. **Hemant Pandit:** Writing – review & editing, Supervision, Funding acquisition, Conceptualization. **Michael G. Bryant:** Writing – review & editing, Supervision, Resources, Funding acquisition, Conceptualization.

Declaration of competing interest

The authors declare that they have no known competing financial interests or personal relationships that could have appeared to influence the work reported in this paper.

Data availability

Data will be made available on request.

Acknowledgements

Funding for this project was received from the UKRI Engineering and Physical Sciences Research Council.

The authors acknowledge the support and funding of the Bragg Centre for Materials Research at the University of Leeds.

References

[1] Wluka Anita E, Ding Changhai, Jones Graeme, Cicuttini Flavia Maria. The clinical correlates of articular cartilage defects in symptomatic knee osteoarthritis: A prospective study. Rheumatology 2005;44(10):1311–6.
[2] Zhao Yiqiong, Fu Dong, Chen Kai, Li Guodong, Cai Zhengdong, Shi Yan, Yin Xiaobing. Outcome of hemiarthroplasty and total hip replacement for active elderly patients with displaced femoral neck fractures: A meta-analysis of 8 randomized clinical trials. PLoS One 2014;9(5):e98071.
[3] McGibbon CA, Krebs DE, Trahan CA, Trippel SB, Mann RW. Cartilage degeneration in relation to repetitive pressure: Case study of a unilateral hip hemiarthroplasty patient. J Arthroplasty 1999;14(1):52–8.
[4] Kim Yee-Suk, Kim Young-Ho, Hwang Kyu-Tae, Choi Il-Yong. The cartilage degeneration and joint motion of bipolar hemiarthroplasty. Int Orthop 2012;36:2015–20.
[5] Pawaskar Sainath Shrikant, Ingham Eileen, Fisher John, Jin Zhongmin. Fluid load support and contact mechanics of hemiarthroplasty in the natural hip joint. Med Eng Phys 2011;33(1):96–105.
[6] Li Junyan, Stewart Todd D, Jin Zhongmin, Wilcox Ruth K, Fisher John. The influence of size, clearance, cartilage properties, thickness and hemiarthroplasty on the contact mechanics of the hip joint with biphasic layers. J Biomech 2013;46(10):1641–7.
[7] Parsons JR. Cartilage. In: Handbook of biomaterial properties. Springer; 1998, p. 40–7.
[8] McCutchen Charles W. The frictional properties of animal joints. Wear 1962;5(1):1–17.
[9] Dowson D, Unsworth A, Wright V. Analysis of 'boosted lubrication'in human joints. J Mech Eng Sci 1970;12(5):364–9.
[10] Ateshian Gerard A. The role of interstitial fluid pressurization in articular cartilage lubrication. J Biomech 2009;42(9):1163–76.
[11] Burris David L, Moore Axel C. Cartilage and joint lubrication: New insights into the role of hydrodynamics. Biotribology 2017;12:8–14.
[12] Krishnan Ramaswamy, Kopacz Monika, Ateshian Gerard A. Experimental verification of the role of interstitial fluid pressurization in cartilage lubrication. J Orthop Res 2004;22(3):565–70.
[13] Ateshian GA. A theoretical formulation for boundary friction in articular cartilage. 1997.
[14] Hargens Alan R, Akeson Wayne H. Stress effects on tissue nutrition and viability. Tissue Nutr Viability 1986;1–24.
[15] Linn Frank C. Lubrication of animal joints: II the mechanism. J Biomech 1968;1(3):193–205.
[16] Linn Frank C. Lubrication of animal joints: I. The arthrotripsometer. JBJS 1967;49(6):1079–98.
[17] Paranjape Chinmay S, Cutcliffe Hattie C, Grambow Steven C, Utturkar Gangadhar M, Collins Amber T, Garrett William E, Spritzer Charles E, DeFrate Louis E. A new stress test for knee joint cartilage. Sci Rep 2019;9(1):2283.
[18] Dedinaite Andra. Biomimetic lubrication. Soft Matter 2012.
[19] Daniel Matej. Role of surface-active lipids in cartilage lubrication. Advances in planar lipid bilayers and liposomes. first ed.. Vol. 15, Elsevier Inc.; 2012, p. 225–43.
[20] Jahn Sabrina, Klein Jacob. Lubrication of articular cartilage. Phys Today 2018;48(71).
[21] Jahn Sabrina, Klein Jacob. Hydration lubrication: The macromolecular domain. Macromolecules 2015;48(15):5059–75.
[22] Ma Liran, Gaisinskaya-kipnis Anastasia, Kampf Nir, Klein Jacob. Origins of hydration lubrication. Nature Commun 2015;8–13.
[23] Spencer Nicholas D. Aqueous lubrication: Natural and biomimetic approaches. Vol. 3, World Scientific; 2014.
[24] Voinier Steven, Moore AC, Benson Jamie M, Price C, Burris David Lawrence. The modes and competing rates of cartilage fluid loss and recovery. Acta Biomater 2022;138:390–7.
[25] Caligaris Matteo, Ateshian Gerard A. Effects of sustained interstitial fluid pressurization under migrating contact area, and boundary lubrication by synovial fluid, on cartilage friction. Osteoarthr Cartil 2008;16(10):1220–7.
[26] Ateshian Gerard A, Wang Huiqun. A theoretical solution for the frictionless rolling contact of cylindrical biphasic articular cartilage layers. J Biomech 1995;28(11):1341–55.
[27] Moore Axel C, Burris David L. Tribological rehydration of cartilage and its potential role in preserving joint health. Osteoarthr Cartil 2017;25(1):99–107.
[28] Graham Brian T, Moore Axel C, Burris David L, Price Christopher. Detrimental effects of long sedentary bouts on the biomechanical response of cartilage to sliding. Connect Tissue Res 2020;61(3–4):375–88.
[29] Kupratis Meghan E, Gure Ahmed E, Benson Jamie M, Ortved Kyla F, Burris David L, Price Christopher. Comparative tribology II–Measurable biphasic tissue properties have predictable impacts on cartilage rehydration and lubricity. Acta Biomater 2022;138:375–89.
[30] Burris DL, Ramsey L, Graham BT, Price C, Moore AC. How sliding and hydrodynamics contribute to articular cartilage fluid and lubrication recovery. Tribol Lett 2019;67:1–10.
[31] Kupratis Meghan E, Gure Ahmed E, Ortved Kyla F, Burris David L, Price Christopher. Comparative tribology: Articulation-induced rehydration of cartilage across species. Biotribology 2021;25:100159.
[32] Putignano Carmine, Burris David, Moore Axel, Dini Daniele. Cartilage rehydration: The sliding-induced hydrodynamic triggering mechanism. Acta Biomater 2021;125:90–9.
[33] Spiller Kara L, Maher Suzanne A, Lowman Anthony M. Hydrogels for the repair of articular cartilage defects. Tissue Eng B: Rev 2011;17(4):281–99.
[34] Qiu Fei, Fan Xiaopeng, Chen Wen, Xu Chunming, Li Yumei, Xie Renjian. Recent progress in hydrogel-based synthetic cartilage: Focus on lubrication and load-bearing capacities. Gels 2023;9(2):144.
[35] Kanca Yusuf, Milner Piers, Dini Daniele, Amis Andrew A. Tribological properties of PVA/PVP blend hydrogels against articular cartilage. J Mech Behav Biomed Mater 2018;78:36–45.
[36] Murakami Teruo, Sakai Nobuo, Yamaguchi Tetsuo, Yarimitsu Seido, Nakashima Kazuhiro, Sawae Yoshinori, Suzuki Atsushi. Evaluation of a superior lubrication mechanism with biphasic hydrogels for artificial cartilage. Tribol Int 2015;89:19–26.
[37] Maher SA, Doty SB, Torzilli PA, Thornton S, Lowman AM, Thomas JD, Warren R, Wright TM, Myers E. Nondegradable hydrogels for the treatment of focal cartilage defects. J Biomed Mater Res A: Off J Soc Biomater Jpn Soc Biomater Aust Soc Biomater Korean Soc Biomater 2007;83(1):145–55.
[38] Mancini Irina AD, Vindas Bolaños Rafael A, Brommer Harold, Castilho Miguel, Ribeiro Alexandro, Van Loon Johannes PAM, Mensinga Anneloes, Van Rijen Mattie HP, Malda Jos, van Weeren René. Fixation of hydrogel constructs for cartilage repair in the equine model: A challenging issue. Tissue Eng C: Methods 2017;23(11):804–14.
[39] Liu Hui, Zhao Xiaoduo, Zhang Yunlei, Ma Shuanhong, Ma Zhengfeng, Pei Xiaowei, Cai Meirong, Zhou Feng. Cartilage mimics adaptive lubrication. ACS Appl Mater Interfaces 2020;12(45):51114–21.
[40] Lin Weifeng, Klein Jacob. Recent progress in cartilage lubrication. Adv Mater 2021;33(18):2005513.
[41] Ishihara Kazuhiko. Highly lubricated polymer interfaces for advanced artificial hip joints through biomimetic design. Polym J 2015;47(9):585–97.
[42] Liu Guoqiang, Feng Yang, Zhao Nan, Chen Zhuo, Shi Junqin, Zhou Feng. Polymer-based lubricating materials for functional hydration lubrication. Chem Eng J 2022;429:132324.
[43] Kobayashi Motoyasu, Takahara Atsushi. Tribological properties of hydrophilic polymer brushes under wet conditions. Chem Record 2010;10(4):208–16.
[44] Kyomoto Masayuki, Moro Toru, Saiga Ken-ichi, Miyaji Fumiaki, Kawaguchi Hiroshi, Takatori Yoshio, Nakamura Kozo, Ishihara Kazuhiko. Lubricity and stability of poly (2-methacryloyloxyethyl phosphorylcholine) polymer layer on Co–Cr–Mo surface for hemi-arthroplasty to prevent degeneration of articular cartilage. Biomaterials 2010;31(4):658–68.
[45] Elkington Robert J, Hall Richard M, Beadling Andrew R, Pandit Hemant, Bryant Michael G. Highly lubricious SPMK-g-PEEK implant surfaces to facilitate rehydration of articular cartilage. J Mech Behav Biomed Mater 2023;106084.
[46] Yu Yunlong, Cirelli Marco, Li Pengfei, Ding Zhichao, Yin Yue, Yuan Yucheng, De Beer Sissi, Vancso G Julius, Zhang Shiyong. Enhanced stability of poly (3-sulfopropyl methacrylate potassium) brushes coated on artificial implants in combatting bacterial infections. Ind Eng Chem Res 2019;58(47):21459–65.
[47] Elkington Robert J, Hall Richard M, Beadling Andrew R, Pandit Hemant, Bryant Michael G. Brushing up on cartilage lubrication: Polyelectrolyte-enhanced tribological rehydration. Langmuir 2024.
[48] Elkington Robert, Beadling Andrew, Hall Richard, Pandit Hemant, Bryant Michael. Biomimetic highly lubricious polyelectrolyte functionalized peek surfaces for novel hemiarthroplasty implants and focal resurfacing. In: Orthopaedic proceedings. Vol. 103, Bone & Joint; 2021, p. 34, (SUPP_16).
[49] Kobayashi Motoyasu, Takahara Atsushi. Tribological properties of hydrophilic polymer brushes under wet conditions. Chem Record 2010;10(4):208–16.
[50] Kobayashi Motoyasu, Takahara Atsushi. Polyelectrolyte brushes : A novel stable lubrication system in aqueous conditions. 2012, p. 403–12. http://dx.doi.org/10.1039/c2fd00123c.
[51] Hodge WA, Harris WH. Contact pressures in the human hip joint measured in vivo. 1986;83(May):2879–2883.

[52] Brand Richard A. Joint contact stress: A reasonable surrogate for biological processes? Iowa Orthop J 2005;25:82.
[53] Tanaka Eiji, Iwabe Tatsunori, Dalla-Bona Diego A, Kawai Nobuhiko, van Eijden Theo, Tanaka Masao, Kitagawa Shoji, Takata Takashi, Tanne Kazuo. The effect of experimental cartilage damage and impairment and restoration of synovial lubrication on friction in the temporomandibular joint. J Orofac Pain 2005;19(4).
[54] Chiang Edward H, Laing Timothy J, Meyer Charles R, Boes Jennifer L, Rubin Jonathan M, Adler Ronald S. Ultrasonic characterization of in vitro osteoarthritic articular cartilage with validation by confocal microscopy. Ultras Med Biol 1997;23(2):205–13.
[55] Federico Salvatore, Herzog Walter. On the anisotropy and inhomogeneity of permeability in articular cartilage. Biomech Model Mechanobiol 2008;7:367–78.
[56] Accardi Mario Alberto, Dini Daniele, Cann Philippa M. Experimental and numerical investigation of the behaviour of articular cartilage under shear loading—interstitial fluid pressurisation and lubrication mechanisms. Tribol Int 2011;44(5):565–78.
[57] Porte Elze, Cann Philippa, Masen Marc. A lubrication replenishment theory for hydrogels. Soft Matter 2020;16(45):10290–300.
[58] Farnham Margot S, Ortved Kyla F, Horner Jeffrey S, Wagner Norman J, Burris David L, Price Christopher. Lubricant effects on articular cartilage sliding biomechanics under physiological fluid load support. Tribol Lett 2021;69:1–14.
[59] Farnham Margot S, Larson Riley E, Burris David L, Price Christopher. Effects of mechanical injury on the tribological rehydration and lubrication of articular cartilage. J Mech Behav Biomed Mater 2020;101:103422.
[60] Forster H, Fisher J. The influence of loading time and lubricant on the friction of articular cartilage. Proc Inst Mech Eng H: J Eng Med 1996;210(2):109–19.
[61] Parkes Maria, Tallia Francesca, Young Gloria R, Cann Philippa, Jones Julian R, Jeffers Jonathan RT. Tribological evaluation of a novel hybrid for repair of articular cartilage defects. Mater Sci Eng: C 2021;119:111495.
[62] Lin Weifeng, Klein Jacob. Hydration lubrication in biomedical applications: From cartilage to hydrogels. Acc Mater Res 2022;3(2):213–23.
[63] Brown CP, Crawford RW, Oloyede Adekunle. An alternative mechanical parameter for assessing the viability of articular cartilage. Proc Inst Mech Eng H: J Eng Med 2009;223(1):53–62.
[64] Farnham Margot S, Ortved Kyla F, Burris David L, Price Christopher. Articular cartilage friction, strain, and viability under physiological to pathological benchtop sliding conditions. Cell Mol Bioeng 2021;14(4):349–63.
[65] Wong M, Carter DR. Articular cartilage functional histomorphology and mechanobiology: A research perspective. Bone 2003;33(1):1–13.
[66] Carter Dennis R, Beaupré Gary S, Wong Marcy, Smith R Lane, Andriacchi Tom P, Schurman David J. The mechanobiology of articular cartilage development and degeneration. Clin Orthop Relat Res® 2004;427:S69–77.
[67] Moore Axel C, Schrader Jordyn Lee, Ulvila Jaclyn J, Burris David L. A review of methods to study hydration effects on cartilage friction. Tribol-Mater Surf Interfaces 2017;11(4):202–14.
[68] Soltz Michael A, Ateshian Gerard A. Experimental verification and theoretical prediction of cartilage interstitial fluid pressurization at an impermeable contact interface in confined compression. J Biomech 1998;31(10):927–34.
[69] Mocny Piotr, Klok Harm Anton. Tribology of surface-grafted polymer brushes. Mol Syst Des Eng 2016;1(2):141–54.
[70] Yang Wufang, Zhou Feng. Polymer brushes for antibiofouling and lubrication. Biosurf Biotribol 2017;3(3):97–114.
[71] Dowson D, Jin Zhong-Min. Micro-elastohydrodynamic lubrication of synovial joints. Eng Med 1986;15(2):63–5.
[72] Medley JB, Dowson D, Wright V. Transient elastohydrodynamic lubrication models for the human ankle joint. Eng Med 1984;13(3):137–51.
[73] de Boer GN, Raske N, Soltanahmadi S, Dowson D, Bryant MG, Hewson RW. A porohyperelastic lubrication model for articular cartilage in the natural synovial joint. Tribol Int 2020;149(May 2019):105760.
[74] Gopinath A, Mahadevan L. Elastohydrodynamics of wet bristles, carpets and brushes. Proc R Soc A: Math Phys Eng Sci 2011;467(2130):1665–85.
[75] Jinpeng Li, Shuyan Yang, Yang Wu, Xinming Li, Feng Guo, Feng Zhou. Correlation between water film thickness and tribological behavior of polymer brush in aqueous lubrication. Tribology 2021;41(6):858–69.
[76] Kobayashi Motoyasu, Tanaka Hiroyoshi, Minn Myo, Sugimura Joichi, Takahara Atsushi. Interferometry study of aqueous lubrication on the surface of polyelectrolyte brush. ACS Appl Mater Interfaces 2014;6(22):20365–71.
[77] Bielecki Robert M, Crobu Maura, Spencer Nicholas D. Polymer-brush lubrication in oil: sliding beyond the stribeck curve. Tribol Lett 2013;49:263–72.
[78] Burris DL, Price LRamsey BTGraham C, Moore AC. How sliding and hydrodynamics contribute to articular cartilage fluid and lubrication recovery. Tribol Lett 2019;67(2):1–10.
[79] Radin Eric L, Swann David A, Weisser Paul A. Separation of a hyaluronate-free lubricating fraction from synovial fluid. Nature 1970;228(5269):377–8.
[80] Walker PS, Dowson D, Longfield MD, Wright Verna. "Boosted lubrication" in synovial joints by fluid entrapment and enrichment. Ann Rheum Dis 1968;27(6):512.
[81] Pradal Clementine, Yakubov Gleb E, Williams Martin AK, McGuckin Michael A, Stokes Jason R. Lubrication by biomacromolecules: Mechanisms and biomimetic strategies. Bioinspiration Biomim 2019;14(5):051001.
[82] Zappone Bruno, Ruths Marina, Greene George W, Jay Gregory D, Israelachvili Jacob N. Adsorption, lubrication, and wear of lubricin on model surfaces: Polymer brush-like behavior of a glycoprotein. Biophys J 2007;92(5):1693–708.
[83] Yarimitsu Seido, Moro Toru, Kyomoto Masayuki, Watanabe Kenichi, Tanaka Sakae, Ishihara Kazuhiko, Murakami Teruo. Influences of dehydration and rehydration on the lubrication properties of phospholipid polymer-grafted cross-linked polyethylene. Proc Inst Mech Eng H: J Eng Med 2015;229(7):506–14.
[84] Abbott Stephen B, De Vos Wiebe M, Mears Laura LE, Cattoz Beatrice, Skoda Maximilian WA, Barker Robert, Richardson Robert M, Prescott Stuart W. Is osmotic pressure relevant in the mechanical confinement of a polymer brush? Macromolecules 2015;48(7):2224–34.
[85] Kobayashi Motoyasu, Terada Masami, Takahara Atsushi. Polyelectrolyte brushes: A novel stable lubrication system in aqueous conditions. Faraday Discuss 2012;156(1):403–12.
[86] Tairy Odeya, Kampf Nir, Driver Michael J, Armes Steven P, Klein Jacob. Dense, highly hydrated polymer brushes via modified atom-transfer-radical-polymerization: Structure, surface interactions, and frictional dissipation. Macromolecules 2015;48(1):140–51.
[87] Ikeuchi K, Fujita S, Ohashi M. Analysis of fluid film formation between contacting compliant solids. Tribol Int 1998;31(10):613–8.